Biochemistry & Analytical Biochemistry
ISSN: 2161-1009

Patel et al., Biochem Anal Biochem 2016, 5:2
DOI; 10.4172/2161-1009.1000265

Research Article Open Access

Interaction between Pyrrolidinium Based Ionic Liquid and Bovine Serum Albumin: A Spectroscopic and Molecular Docking Insight

Rajan Patel[1]*, Meena Kumari[1], Neeraj Dohare[1], Abbul Bashar Khan[1], Prashant Singh[2], Maqsood Ahmad Malik[3] and Amit Kumar[4]

[1]*Biophysical Chemistry Laboratory, Centre for Interdisciplinary Research in Basic Sciences, Jamia Millia Islamia (A Central University), New Delhi, India*
[2]*Department of Chemistry, A. R. S. D. College, University of Delhi, Delhi, India*
[3]*Department of Chemistry, King Abdul Aziz University, Jeddah, Saudi Arabia*
[4]*Centre for Nano and Material Sciences, Jain University, Jain Global Campus, Jakkasandra, Bangalore, India*

Abstract

Herein, we report the interaction of N, N-dimethyl-2-oxopyrrolidinium iodide with bovine serum albumin by using steady-state fluorescence, time-resolved fluorescence, UV-visible and Fourier Transform-Infrared spectroscopy in combination with molecular docking method. The steady state fluorescence spectra results confirmed that N, N-dimethyl-2-oxopyrrolidinium iodide strongly quenches the intrinsic fluorescence of bovine serum albumin by a dynamic quenching mechanism as confirmed by time resolved fluorescence spectroscopy. The thermodynamic parameters (ΔH, ΔG and ΔS) showed that the binding process was spontaneous and enthalpy driven. Moreover, the interacting forces between bovine serum albumin and N, N-dimethyl-2-oxopyrrolidinium were mainly governed through hydrogen bond and van der Waals forces. The Fourier Transform-Infrared spectroscopy results show the conformational change of bovine serum albumin on binding with N, N-dimethyl-2-oxopyrrolidinium. Additionally, molecular modeling results revealed that N, N-dimethyl-2-oxopyrrolidinium binds with the amino acid residues of the sub domain IIA of bovine serum albumin.

Keywords: Ionic liquid; Bovine serum albumin; Fluorescence; FTIR; Quenching; Molecular docking

Abbreviations: DMPI: N, N-Dimethyl-2-Oxopyrrolidinium Iodide; BSA: Bovine Serum Albumin; FTIR: Fourier Transform-Infrared; IL: Ionic Liquid; HAS: Human Serum Albumin; NMR: Nuclear Magnetic Resonance; HPLC: High Performance Liquid Chromatography; LGA: Lamarckian Genetic Algorithm

Introduction

As a biomacromolecule, protein plays vital role in biological system and exhibit varieties of applications. The function of a protein is depends on its native structure. A little disturbance in their microenvironment can alter their native structure and due to this the maintenance of their stability is a big issue for scientific community [1-3]. There are so many factors which affect the stability of protein; however, ligand-protein interaction is one of the most important factors due to the direct binding of the ligand with protein. In many case protein is main target of the drugs when present within the body [4] and come in contact with varieties of ligands like drugs, salts, surfactants, when used in-vitro for research purpose [5]. Therefore, the study of the ligand-protein interaction is necessary to find out the effect of particular ligand on the conformational stability of protein.

Recently, due to various biological applications, the research interest towards ionic liquids (ILs) grown up so rapidly. ILs provided exceptionally interesting solvent media for various biological processes viz. biocatalytic reaction [6] biosensor [7] protein separation, extraction and biopreservation [8,9]. ILs are the solvents that are often liquid at room temperature and consist solely of ions. They have some special unique physiochemical properties like negligible vapor pressure, high thermal stability and large electrochemical window which enhance their role in chemical and biochemical research field [10]. Another fascinating property they have is the diversity in their range which can be easily obtained by substituting the cation-anion pair [11]. Baker et al., reported that 1-butyl-1-methylpyrrolidinium bis (trifluoromethanesulfonyl) imide, ([bmpy][NTf2]), IL provide high thermal stability to the monellin. The onset of thermal unfolding of monellin in [bmpy][NTf2] occurred at 100°C as compared with 40°C in water [12] Also, α-chymotrypsin shows higher thermal stability with ammonium based ILs [13].

In our previous research work we have been reported the interaction of pyrrolidinium based IL (1- Butyl-1-methyl-2-oxopyrrolidinium bromide) with human serum albumin (HSA) and bovine serum albumin (BSA) [14,15]. Therefore, in continuation of our previous work and varieties of useful biological applications of ILs, herein, we have been reporting the binding effect of synthesized IL, N, N-dimethyl-2-oxopyrrolidinium iodide (DMPI) on BSA. The molecular interactions between BSA and DMPI were observed by fluorescence, time resolved fluorescence and UV-visible, FTIR spectroscopic techniques and molecular docking method.

BSA is a serum protein which acts as the major transporter of non-esterified fatty acids, drugs and metabolites to different tissues [16,17]. Due to low cost and easy purification [18,19] as well as structural homology with HSA, [20] BSA is the most studied protein and used as a model in ligand-protein binding. It is a monomeric protein consisting of 582 amino acid residues [21]. The 3-D structure of BSA consists of three homologous domains namely, I, II and III, each of which are further subdivided into two subdomains A and B [22]. Among them, subdomains IIA and IIIA are hydrophobic in nature and serves as principle binding sites. BSA has two tryptophan residues, Trp-212 and Trp-134 located in subdomain IIA and IA respectively. [23].

Materials and Methods

Materials

BSA (96%) was obtained from Sigma Aldrich (code No. A2153)

***Corresponding author:** Rajan Patel, Biophysical Chemistry Laboratory, Centre for Interdisciplinary Research in Basic Sciences, Jamia Millia Islamia (A Central University), New Delhi, India, Tel: +91-8860634100; E-mail: rpatel@jmi.ac.in

Received: February 08, 2016; **Accepted:** April 18, 2016; **Published** April 21, 2016

Citation: Patel R, Kumari M, Dohare N, Khan AB, Singh P, et al. (2016) Interaction between Pyrrolidinium Based Ionic Liquid and Bovine Serum Albumin: A Spectroscopic and Molecular Docking Insight. Biochem Anal Biochem 5: 265. doi:10.4172/2161-1009.1000265

and was used without further purification. All BSA solutions were prepared in sodium phosphate buffer solution of pH 7.40. Doubly distilled water was used throughout the experiments. The schematic diagram of DMPI was shown in scheme 1. DMPI was synthesized by using the following process: (Scheme 1)

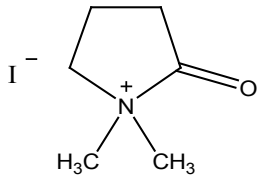

Scheme 1: Schematic diagram of N,N-dimethyl-2-oxopyrrolidonium iodide.

Synthesis of DMPI

A three-necked round bottom flask (250 ml) was flushed with nitrogen gas and charged with 1 mol (1 equiv) of freshly distilled N-methyl pyrrolidone, 100 mL of acetonitrile and 1.1 mol (1.1 equiv) of 1-iodomethane and brought to a gentle reflux (75-80°C internal temperature). Then the solution was heated under reflux for 26 hours and then cooled to room temperature (30°C). The volatile material was removed from the resulting yellow solution under reduced pressure to afford the IL. The afforded product was well characterized by 1H NMR, 13C NMR, FTIR techniques. The purity of the synthesized ionic liquid was checked using HPLC. FTIR (ν=cm^{-1}): 2912.19, 1712.75, 1398.10, 1346.76 and 879.28; NMR (δ, $CdCl_3$): ^{1}H-NMR aliphatic proton at C_3 (2.36, 2H); aliphatic proton at C_4 (2.04, 2H); aliphatic proton at C_5 (3.09, 2H); aliphatic proton at $C_{1'}$ & $C_{1''}$ (2.89, 4H); ^{13}C-NMR aliphatic carbon are 56.1, 49.8, 34.1, 28.1 and carbonyl carbon at 181.5; HPLC purity of the synthesized IL is 93.1%.

Methods

Fluorescence spectroscopy

The fluorescence spectra were recorded on a Cary Eclipse spectrofluorimeter (Varian, USA) equipped with a 150W xenon lamp. The intrinsic fluorescence of the BSA was measured at an excitation wavelength of 280 nm with both excitation and emission band-width of 5 nm. The fluorescence spectra was recorded at three temperatures; 298, 308 and 318 K which was controlled by using constant-temperature cell holder connected to constant-temperature water circulator (Varian, USA). Synchronous fluorescence spectra were acquired by the same spectroflourimeter. The difference between excitation and emission wavelength was kept constant ($\Delta\lambda = \lambda_{em} - \lambda_{ex}$). The Δλ at 15 nm and 60 nm showed by synchronous fluorescence spectra gives characteristic information of Tyrosine (Tyr) and Tryptophan (Trp) residues, respectively with the excitation and emission slit widths at 5 nm.

Correction for inner filter effect

The fluorescence data was corrected in order to eliminate the effect produce due to absorption of light at excitation wavelength (λ_{ex}) and emission wavelength (λ_{em}) by DMPI in solution (i.e., inner filter effect) so that the actual quenching effect of binding of DMPI with BSA can be obtained. The absorbance of titrated solutions (for each concentration of DMPI at $\Delta\lambda_{ex}$ (280 nm) and $\Delta\lambda_{em}$ (346 nm) were recorded and the corrected fluorescence was estimated by using the following eqn [24].

$$F_{corr} = F_{obs}\, 10^{(A_{ex}+A_{em})/2} \quad (1)$$

Where F_{corr} and F_{obs} are corrected and experimentally measured fluorescence intensities respectively, A_{ex} and A_{em} is the measured change in absorbance at λ_{ex} (280 nm) and λ_{em} (346 nm) of DMPI.

Time-resolved fluorescence spectroscopy

Fluorescence lifetimes measurements were performed using a single-photon counting spectrometer equipped with pulsed nanosecond LED excitation heads at 280 nm (Horiba, Jobin Yvon, IBH Ltd, Glasgow, UK) at room temperature. The lifetime data were measured to 10,000 counts in the peak, unless otherwise indicated. The excitation and emission wavelengths were set at 280 and 342 nm respectively. The instrumental response function was recorded sequentially using a scattering solution and a time calibration of 114 ps/channel. All experiments were performed using excitation and emission slits with a band pass of 8 nm. The goodness of fit was judged in terms of both a chi-squared (χ^2) value and weighted residuals. Data were analysed using a sum of exponentials, employing a nonlinear least squares reconvolution analysis from Horiba (Jobin Yvon, IBH Ltd). The impulse response functions (IBH DAS6 software) were used to analyze decay curves. The Mean fluorescence lifetimes <τ> for bi-exponential iterative fittings were calculated by using the following relation [24]:

$$\langle \hat{o} \rangle = \frac{\sum a_i \hat{o}_i^{\,2}}{\sum a_i \hat{o}_i} \quad (2)$$

Where a_i and τ_i are the relative contribution and life time of different components to the total decay.

UV-vis spectrophotometry

The UV-vis spectra of BSA-DMPI were measured using the Analytik Jena Specord-250 spectrophotometer (USA). Quartz cuvettes having 1 cm path length were used for the measurements. The absorption spectra of BSA were recorded at different IL concentration at λ_{280} nm. The absorbance was measured by keeping constant concentration of BSA (5 μM) and varying the concentrations of the DMPI. The experiments were recorded at 298 K.

FTIR Spectroscopy

FTIR spectra were measured with a Specac Golden Gate diamond ATR sampler fitted to a Bruker Tensor 27 with an MCT detector. Approximately 10 μl of 150 μM BSA solution was pipette out onto a diamond window and a 100 scan interferogram was collected in single beam mode, with 2 cm^{-1} resolution, from 1400 to 1800 cm^{-1}. Reference spectra were recorded under identical conditions with only the solvent media. The subtraction of the reference spectrum was carried out in accord with the criteria described by Maurya et. al. [25].

Molecular docking

Molecular docking was performed to determine the possible binding mode of DMPI with BSA. The crystal structure of BSA (PDB ID: 4F5S) was obtained from the Protein Data Bank. The 3-D structure of DMPI was generated by using 3D Chem Draw Ultra 8.0 software. The docking experiments were performed using the molecular docking software AutoDock4.2 [26]. The possible binding conformation of the DMPI with BSA was computed by using LGA implemented in Auto Dock. Additionally, docking was performed by setting the grid volume as 60 × 50 × 80 Å with 0.375 Å grid spacing. The grid center was set as 22.556, 35.519, 97.262 Å. Each docking experiment was derived from 10 different runs that were set to terminate after a maximum of 2.5×10^6 energy evaluations. The population size was set to 150. The lowest energy conformation was utilized for further analysis.

Results and Discussion

Fluorescence spectroscopy

The fluorescence spectrum is highly sensitive for change in

micropolarity of environment in the vicinity of fluorophore molecule and hence, widely used for studying the ligand-protein binding [27,28]. The proteins have three aromatic amino acid residues viz: tryptophan (Trp), tyrosine (Tyr) and phenylalanine (Phe) which acts as intrinsic fluorophore due to presence of π bonds. The fluorescence emission was recorded at an excited wavelength (λ_{ex}) of 280 nm by keeping constant concentration of BSA (5 μM) and varying concentration of DMPI (1.07-18.51 mM). As shown in Figure 1, BSA give an fluorescence emission band at 346 nm which was continuously decrease with increasing concentration of DMPI, indicated that DMPI quenched the fluorescence of intrinsic fluorophore of BSA. Also, a blue shift was observed from 346 to 328 nm in the fluorescence emission of BSA, with increasing concentrations of DMPI, which arise due the change in conformation of BSA that shifts the Trp residues towards a more hydrophobic environment [29] .

Fluorescence quenching decreases the fluorescence intensity of a fluorophore due to variety of molecular interactions namely excited state reactions, energy transfer, molecular rearrangements, and ground state complex formation [24,30]. Usually the fluorescence quenching is classified as dynamic quenching and static quenching. Dynamic quenching results from collision between the fluorophore and quencher, while static quenching results from the formation of a ground-state complex between the fluorophore and quencher. In static quenching, the increase in temperature decreases the binding constant due to reduced stability of complex, on contrary the dynamic quenching, is marked by the increase in the binding constant at higher temperatures which leads to increase in collision [31]. The quenching mechanism is

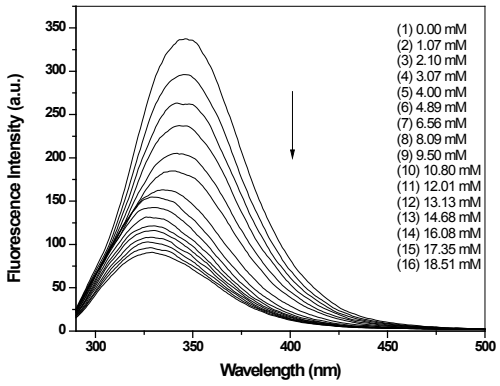

Figure 1: (a) Fluorescence quenching spectra of BSA (5 μM) with different concentrations of DMPI at 298 K and pH 7.4.

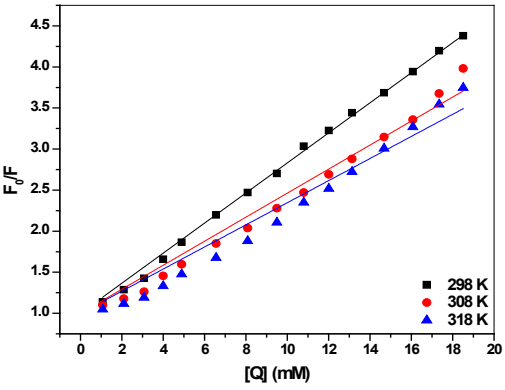

Figure 2: Stern-Volmer plots of BSA at different concentrations of DMPI at different temperature (298, 308 and 318 K).

Temp. (K)	K_q (10^{10} L mol^{-1} s^{-1})	R^2
298	1.83	0.999
308	1.46	0.997
318	1.35	0.994

Table 1: Stern–Volmer quenching constants (K_q) of BSA-DMPI system at different temperatures (pH = 7.4, λ_{ex} = 280 nm).

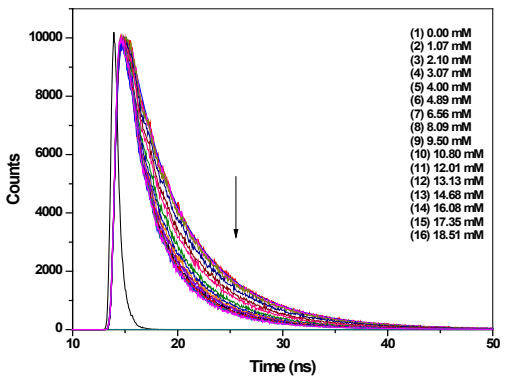

Figure 3: Time-resolved fluorescence decay of BSA-DMPI system at 298 K and pH 7.40.

deduced by the Stern–Volmer plot (Figure 2). The fluorescence intensity was corrected to eliminate the inner filter effect by applying Equation 1. The following Stern–Volmer equation describes the quenching process as follows [32]:

$$\frac{F_0}{F} = 1 + K_{SV}[Q] = 1 + K_q \tau_o [Q] \quad (3)$$

Where, F_0 and F are the fluorescence intensities in the absence and presence of quencher, K_{sv} is the Stern-Volmer quenching constant, [Q] is the concentration of quencher, k_q is the bimolecular quenching rate constant and τ_0 is the average life time of molecules in the absence of DMPI and its value is about 10^{-8} s [24]. The K_{sv} values are obtained from the slope of the Stern-Volmer plot for BSA-DMPI system at different temperature (Figure 2). The values of quenching rate constant (K_q) obtained from the ratio K_{sv}/τ_0 (Table 1), was found to be similar to the maximum collision quenching rate constant of various kinds of biomolecule (2.0 ×10^{10} L mol^{-1} s^{-1}) [24], suggested the involvement of dynamic quenching mechanism in the interaction process. The quenching mechanism involved in the BSA-DMPI system was further conformed by time resolved and UV-vis spectroscopy.

Time resolved spectra

Fluorescence lifetime of the fluorophore is sensitive to the ligand-protein interaction and frequently used for precise determination of the quenching mechanism. It is very sensitive towards excited state interactions because ground state complex formation results in reduction in the total number of fluorophore molecules rather affecting their life time in excited state [33]. Therefore, this technique was utilized for validating the quenching results obtained from steady state fluorescence spectroscopy. Figure 3 shows the fluorescence decay curve of BSA at different concentrations of DMPI. As the data was fitted by using the biexponential function, the average lifetime (τ_{av}) was used for analysing the results. The values of fluorescence lifetimes and statistical parameters are represented in Table 2. The value of τ_{av} obtained for pure BSA is close to the value reported earlier [14]. It was found that the τ_{av} of BSA decrease continuously with increasing concentrations of DMPI. This shows that DMPI makes collisional interactions with BSA and quenches the

fluorophore of BSA through dynamic mechanism. These results confirmed the involvement of dynamic quenching mechanism in the interaction system. The similar result was observed from steady state spectra.

Binding parameters

The fluorescence data of BSA in presence of various concentrations of DMPI is further used for calculation of binding parameters such as binding constant and number of binding site. The binding constant and binding sites were calculated from the following equation [30]:

$$\log \frac{F_0 - F}{F} = \log K_a + n\log[Q] \quad (4)$$

Where K_b and n are the binding constant and number of binding sites, respectively. The plot of log F_0-F/F versus log [Q] at three different temperatures gives a straight line shown in Figure 4. The values of K_b and n are calculated from intercept and slope of the double log plot and are listed in Table 3. The value of regression coefficient is also shown which is nearly equal to one. From Table 3 there is a small change in K_b value is observed with increase in temperature which suggests that the stability of BSA-DMPI complex decreases with increasing temperature.

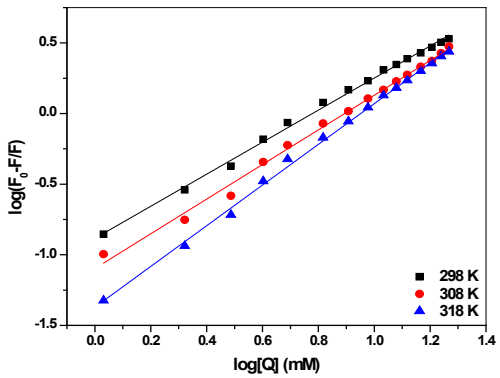

Figure 4: The plots of log (F_0-F)/F versus log [Q] for quenching of BSA by DMPI at different temperatures.

[DMPI]	τ_1 (ns)	a_1	τ_2	a_2	$\tau_{av.}$	τ_0/τ
0.00	2.86	19.49	6.61	80.51	6.25	1.00
1.07	2.44	15.45	6.34	84.55	6.08	1.02
2.10	2.11	14.00	6.19	86.00	5.98	1.04
3.07	2.06	15.42	5.99	84.58	5.76	1.08
4.00	1.80	16.52	5.65	83.48	5.42	1.15
4.89	1.80	19.26	5.47	80.74	5.20	1.20
6.56	1.79	25.01	5.30	74.99	4.95	1.26
8.09	1.77	29.65	5.25	70.35	4.82	1.29
9.50	1.75	32.56	5.23	67.44	4.75	1.31
10.80	1.74	35.36	5.23	64.64	4.69	1.33
12.01	1.76	37.85	5.23	62.15	4.64	1.34
13.13	1.73	38.97	5.16	61.03	4.56	1.37
14.68	2.34	49.22	5.32	50.78	4.43	1.40
16.08	2.36	52.31	5.32	47.69	4.35	1.43
17.35	2.42	56.90	5.44	43.10	4.32	1.44
18.51	2.40	57.44	5.41	42.56	4.28	1.46

τ_1 and τ_2 = fluorescence lifetime for the fast and the slow components in the exponential decay; α_1 and α_2 pre-exponential factor (amplitude) for the fast and the slow components in the exponential decay.

Table 2: Fluorescence lifetime of BSA and BSA-DMPI system as function of DMPI concentration at 298 K and pH 7.4.

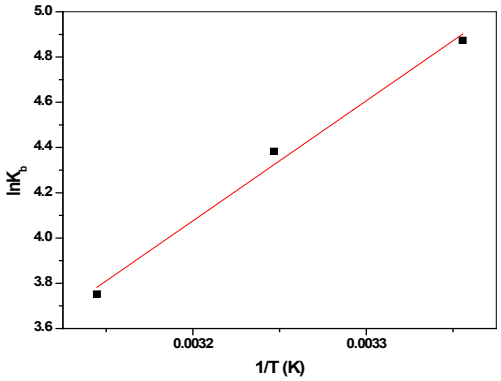

Figure 5: Vant Hoff's plot for the interaction of BSA and DMPI at different temperatures (298, 308 and 318 K).

Temp. (K)	K_a (10^2 L mol^{-1})	n	ΔH (kJ mol^{-1})	ΔS (J mol^{-1}K^{-1})	ΔG (kJ mol^{-1})	R^2
298	1.31	1.13	-44.11	-107.26	-12.14	0.997
308	0.80	1.23			-11.07	0.994
318	0.43	1.44			-10.00	0.998

K_a = Binding constant; n = Number of binding sites; ΔH = Enthalpy change; ΔS = Entropy change; ΔG = Free energy change.

Table 3: The binding parameters of BSA-DMPI interaction at pH 7.4.

Also there is a small variation in the value of ΔG The value of n which is nearly equals to 1 indicates that DMPI shows 1:1 binding with BSA.

Thermodynamic parameter and nature of the binding forces

The thermodynamic parameters, enthalpy change (ΔH) and entropy change (ΔS) of BSA-DMPI interaction were calculated in order to determine the binding modes and the forces involved in binding process. The value of ΔH and ΔS determined by the following van't Hoff equation [32].

$$\ln K_a = -\frac{\Delta H}{RT} + \frac{\Delta S}{R} \quad (5)$$

where K_b is the binding constant analogous to the Stern–Volmer quenching constants K_{sv} at the corresponding temperature, R is the gas constant and T is the experimental temperature. The values of ΔH and ΔS of the BSA-DMPI system were obtained from the slope and the intercept of van't Hoff plot (Figure 5) respectively. The free energy change (ΔG) is estimated from the following relationship:

$$\Delta G = \Delta H - T\Delta S \quad (6)$$

The values thus obtained are summarised in Table 3. The negative value of ΔG, ΔS and ΔH are obtained for the BSA-DMPI interaction. Negative values of ΔG suggested the spontaneity of the interaction process. Negative values of ΔS and ΔH indicated that hydrogen bond and van der Waals forces play major role in binding process. Also the negative value of ΔH suggests that the binding process is enthalpy driven and exothermic in nature [32]. Moreover, from Table 3 it was observed that the value of ΔG decrease slightly with temperature, which again support the variation in the value of K_b with temperature ie. on increasing temperature the binding between HSA and DMPI is less. The value of ΔG observed experimentally was consistent with the value observed from docking study.

Synchronous fluorescence spectra

Synchronous fluorescence is sensitive to the change in microenvironment of fluorophore residues hence give information

about the conformation of protein [34]. The shift in maximum emission wavelength of fluorophore residue correlates the change in polarity and conformation of protein [35]. Synchronous spectra offer the characteristic information of Tyr and Trp residues when the Δλ fixed between excitation and emission wavelength at 15 nm and 60 nm respectively [24]. Figure 6 shows the synchronous fluorescence spectra of BSA as a function of DMPI concentration at 298 K. As shown in Figures 6 a and 6 b the fluorescence intensity at Δλ = 60 nm is greater than the Δλ = 15 nm which suggest that intrinsic fluorescence of BSA is largely contributed by Trp residues. Also, the decrease in fluorescence intensity with addition of DMPI shows that presence of DMPI leads to fluorescence quenching of BSA while more effect is observed for Trp residue. The blue shift in maximum emission wavelength of BSA at Δλ = 15 nm indicate that binding of DMPI affect the microenvironment of Tyr residue.

UV-vis absorption spectra

UV-Vis spectroscopy provides useful insight about the ligand-protein interaction and change in protein conformation [36]. This technique is also used for distinguishing the static and dynamic quenching. The shift in absorbance spectrum of fluorophore with addition of ligand signifies the static quenching and vice versa [37]. Herein, the absorptions spectra of BSA at different concentration of DMPI were recorded for understanding the quenching mechanism. As shown in Figure 7, there is a strong absorption band at about 278 nm can provide us the information about three buried aromatic amino acids (i.e., Trp, Tyr, and Phe). It was observed that the absorption spectra of BSA at 278 nm (Figure 7) remains almost unchanged with the addition of the DMPI (1.07-18.5 mM) which suggests that DMPI makes collisional interaction rather forming the complex in ground state of fluorophore [38]. These results provide evidence of dynamic quenching for BSA-DMPI interaction system and are in good agreement with the results obtained from time resolved and steady state fluorescence spectroscopy.

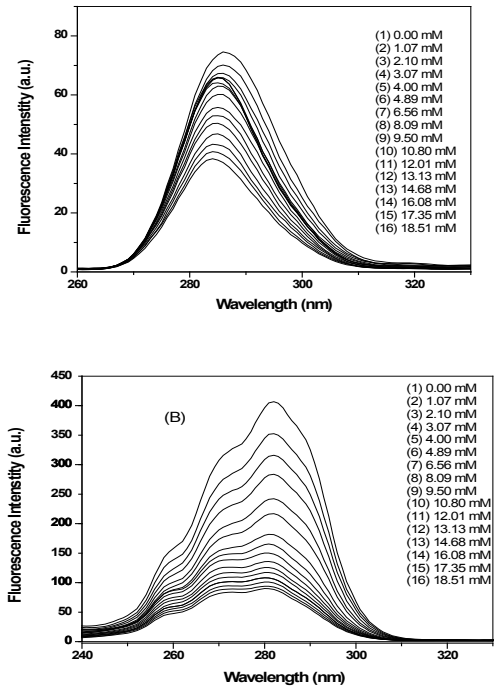

Figure 6: Synchronous fluorescence spectra of BSA as a function of DMPI concentration (A) Δλ =15 nm; (B) Δλ =60 nm, (T=298 K, pH=7.4).

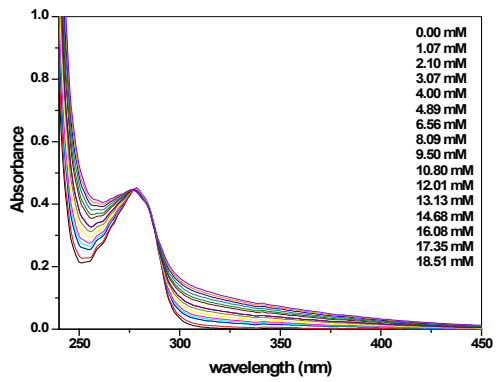

Figure 7: UV-VIS spectra of BSA as a function of DMPI concentration at 298 K and pH 7.40.

FTIR spectroscopy

The FTIR spectra of BSA were monitored to visualize the conformational changes at the secondary structural level in protein in a specified range from 1500 to 1700 cm^{-1}. Two strong bands one at ≈1653 cm^{-1} while other at ≈1548 cm^{-1} is assigned for amide I and amide II bands, respectively. The sensitivity of amide I band (≈1653 cm^{-1}) is mainly attributed to the C=O stretching vibration of amide group of protein, while the amide II band (≈1548 cm^{-1}) arises due to N–H deformation and C–N stretching [39,40]. These two bands were utilized to monitor the pattern of hydrogen bonds and the secondary structure of proteins different conditions. The shift in amide bands was exploited to monitor the formation of hydrogen bonds between the N–H and C=O of the BSA amide bonds and water molecules. The amide I band is more sensitive to the secondary structure of the protein and have higher signal intensity than amide II band [41]. The several overlapping vibrations in the following range (1700-1600 cm^{-1}) were assigned to amide I band depicts combinations of secondary structure conformations like β-sheet (1638-1610cm^{-1}), random coil (1648-1638 cm^{-1}), α-helix (1660–1650cm^{-1}), turns (1680–1660 cm^{-1}) and β-antiparallel (1692-1680) [42,43].

Herein, the difference spectrum of BSA was utilized for observing the change in the secondary structure of BSA in the presence of DMPI. The Figure 8 (A to F) shows difference spectra of BSA at various concentration of DMPI ranging from 0 to 18.5 mM. From Figure 8 it was observed that both of the amide I and II bands were affected with the addition of DMPI. Quite, a well-known fact, amide I band is more sensitive to the secondary structure of the protein [44,45]; it was further employed for quantitative analysis of the secondary structure of BSA. The peak positions in the spectral region 1700-1600 cm^{-1} of amide I bands were deconvoluted, adjusted and the area was measured with the Gaussian function fitting curves. The area of all component bands assigned to a given conformation was then summed up and divided by the total area. For all the fittings, the coefficient of determination (R^2) was 0.989 and 0.996±0.002 for BSA and BSA-DMPI complex, respectively. The spectra of free BSA obtained were found to be similar with the reported data after curve fitting [14,46]. As shown in Figures 8a - 8f, the helical content of the secondary structure of BSA was decreased in the presence of DMPI while, the β-sheet and β-turn was increases at 1.07-10.80 mM DMPI concentration range. The decrease in helical content and increase in β-structure implies partial unfolding of BSA up to this concentration range [47]. A greater decrease in helical content and increase in β-structure and random coil was observed at 18.51 mM [DMPI] which suggests the further unfolding of BSA [47]. It

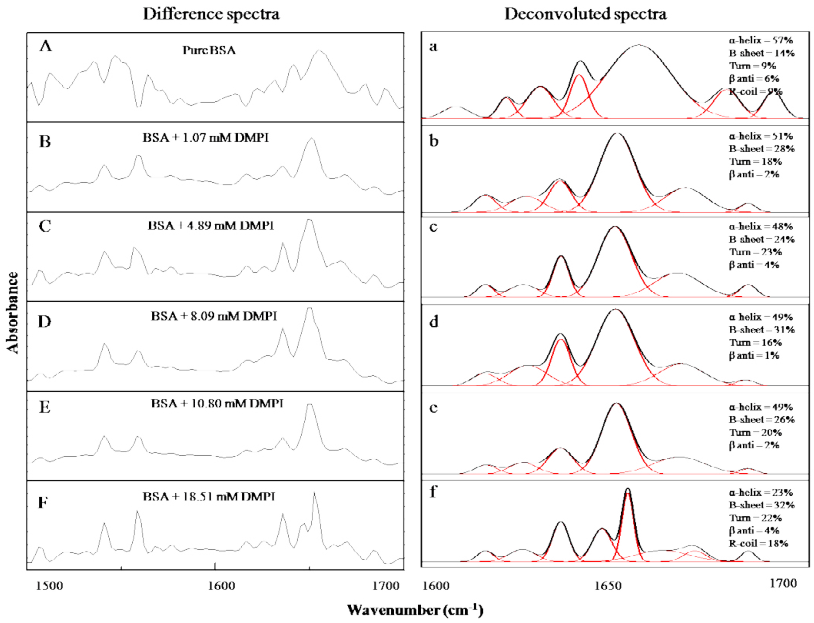

Figure 8: FT-IR and deconvoluted spectra of BSA in presence of DMPI. The A and to F and concentrations of DMPI are 0, 1.07, 4.89, 8.09, 10.80 and 18.51 mM and that of BSA is 100 μM. The difference spectra are assigned by capital letters and their respective deconvoluted spectra are assigned by small latter.

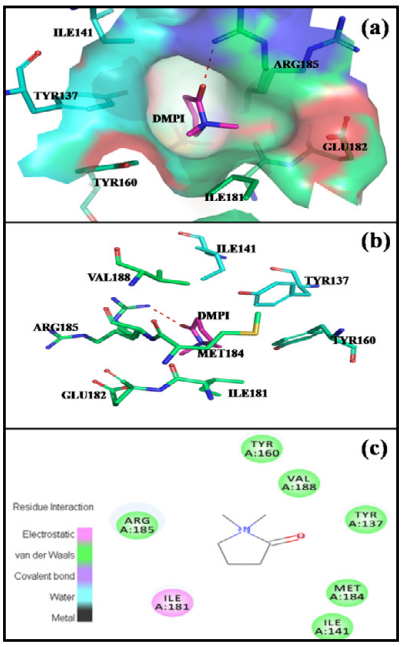

Figure 9: Schematic representation of BSA-DMPI docked structure. (a) Surface view of the docked DMPI with BSA showing residues (sticks) ILE141, TYR137, TYR160, ILE181, GLU182 and ARG185 at the entry site of the cavity. The image was visualized using PyMol. (b) docked DMPI (represented by magenta coloured stick) and neighbouring amino acid residues (represented by cyan and green coloured sticks) of BSA. The red coloured dots between ARG185 residue of BSA and O atom of DMPI representing hydrogen bond between them. (c) Graphical representation of BSA docked with DMPI showing van der Waals interactions with ARG185, TYR160, VAL188, TYR137, MET184, ILE141 and electrostatic interaction with ILE181. The image was visualized using discovery studio.

was inferred from above discussed results that DMPI have destabilizing effect on structural stability of BSA, it shifts BSA from its folded state to unfolded state.

Molecular docking analysis

Like *in vitro* study, the *in-silico* study also helpful for understanding the ligand-protein interaction. Here, the molecular docking is used for determining the BSA-DMPI interaction as an additional tool for supporting the experimental results. The docking was performed by using the molecular docking software AutoDock4.2 as discussed in material section. Out of 10 conformers obtained, the lowest binding energy (-14.44 kJ) conformer is selected for analyzing the results. It was reported that BSA contains two principle ligand binding sites namely, site I and site II in hydrophobic cavity of subdomain IIA and IIIA respectively [48].

The lowest energy ranked model with most possible interaction between DMPI and BSA is shown in Figure 9. As shown in Figure 9 the DMPI bind within the hydrophobic pocket of subdomain IIA surrounded by hydrophobic, positively and negatively charged residues namely, ILE141, TYR137, TYR160, ILE181, ARG185 and GLU182. The results show that binding between DMPI and BSA is occurs mainly through hydrogen bonding, electrostatic and van der Waals interactions that supports the experimental results. The free energy of binding obtained from docking results is also nearly equals to the experimental value, which suggest spontaneity of binding process. The direct involvement of Tyr residue in binding and formation of hydrogen bonds clearly support the fluorescence quenching and shifting of fluorophore residues (Tyr) towards more hydrophobic environment on binding with DMPI. These results also support our conclusion from synchronous fluorescence spectra.

Conclusion

The interaction between DMPI and BSA was studied using fluorescence, time resolved, UV-vis and FTIR spectroscopic techniques. Furthermore, molecular docking study provided accurate insights regarding the binding of DMPI with BSA. The results obtained from different techniques shows that DMPI bind with BSA near Trp and Tyr residues and quenched these fluorophores through dynamic quench-

ing mechanism. It was observed that DMPI has single binding site on BSA and binds in the hydrophobic pocket of subdomain IIA. It was also observed that the increase in temperature decrease the stability of complex. The obtained thermodynamic parameters shows that the binding reaction is spontaneous, exothermic and enthalpy driven and hydrogen bonds and van der Waals forces play major role in DMPI-BSA binding. FTIR results show that, DMPI suppress conformational stability of BSA by shifting the native folded form of BSA toward non-native unfolded form. In addition, the molecular docking results are in good agreements with experimental results.

Acknowledgment

Dr. Rajan Patel thanks to Science and Engineering Research Board (SERB), New Delhi for providing research grant with Sanction Order No. (SR/S1/PC-19/2011). One of the authors (Meena Kumari) is also thank full to CSIR, New Delhi for SRF fellowship.

References

1. Klibanov AM (1983) Stabilization of enzymes against thermal inactivation. Adv Appl Microbiol 29: 1-28.
2. Illanes A (1999) Stability of biocatalysts. Electron J Biotechnol 2: 1-9.
3. Volkin DB, Klibanov AM (1989) Protein function: Practical approach, IRL Press, Oxford.
4. Cui FL, Fan J, Li JP, Hu ZD (2004) Interactions between 1-benzoyl-4-p-chlorophenyl thiosemicarbazide and serum albumin: investigation by fluorescence spectroscopy. Bioorg Med Chem 12: 151-157.
5. Prieto G, Sabín J, Ruso JM, González-Pérez A, Sarmiento F (2004) A study of the interaction between proteins and fully-fluorinated and fully-hydrogenated surfactants by ?-potential measurements. Colloids Surf A Physicochem Eng Asp 249: 51-55.
6. Suresh kumar M, Lee CK (2009) Biocatalytic reactions in hydrophobic ionic liquids. J Mol Catal B Enzym 60: 1-12.
7. Ohno H, Suzuki C, Fukumoto K, Yoshizawa M, Fujita K (2003) Electron transfer process of poly(ethylene oxide)-modified cytochrome c in imidazolium type ionic liquid. Chemistry letters 32: 450-451.
8. Pei Y, Wang J, Wu K, Xuan X, Lu X (2009) Ionic liquid-based aqueous two-phase extraction of selected proteins. Sep Purif Technol 64: 288-295.
9. Dreyer S, Salim P, Kragl U (2009) Driving forces of protein partitioning in an ionic liquid-based aqueous two-phase system. Biochem Eng J 46: 176-185.
10. Patel R, Kumari M, Khan AB (2014) Recent advances in the applications of ionic liquids in protein stability and activity: a review. Appl Biochem Biotechnol 172: 3701-3720.
11. Freemantle M (1998) Designer solvents. Chemical & Engineering News Archive 76: 32-37.
12. Baker SN, McCleskey TM, Pandey S, Baker GA (2004) Fluorescence studies of protein thermostability in ionic liquids. Chem Commun (Camb) : 940-941.
13. Attri P, Venkatesu P (2013) Exploring the thermal stability of a-chymotrypsin in protic ionic liquids. Process Biochem 48: 462-470.
14. Kumari M, Maurya JK, Singh UK, Khan AB, Ali M, et al. (2014) Spectroscopic and docking studies on the interaction between pyrrolidinium based ionic liquid and bovine serum albumin. Spectrochim Acta A Mol Biomol Spectrosc 124: 349-356.
15. Kumari M, Maurya JK, Tasleem M, Singh P, Patel R (2014) Probing HSA-ionic liquid interactions by spectroscopic and molecular docking methods. J Photochem Photobiol B 138: 27-35.
16. Hierrezuelo JM, Nieto-Ortega B, Ruiz CC (2014) Assessing the interaction of hecameg with bovine serum albumin and its effect on protein confermation: Aspectroscopic study. J Lumin 147: 15-22.
17. Liu J, Tian J, Tian X, Hu Z, Chen X (2004) Interaction of isofraxidin with human serum albumin. Bioorg Med Chem 12: 469-474.
18. Carter DC, Ho JX (1994) Structure of serum albumin. Adv Protein Chem 45: 153-203.
19. Carter DC, Chang B, Ho JX, Keeling K, Krishnasami Z (1994) Preliminary crystallographic studies of four crystal forms of serum albumin. Eur J Biochem 226: 1049-1052.
20. Li X, Wang G, Chen D, Lu Y (2014) Binding of ascorbic acid and □-tocopherol to bovine serum albumin: a comparative study. Mol Biosyst 10: 326-337.
21. Maruyama T, Katoh S, Nakajima M, Nabetani H, Abbott TP, et al. (2001) FT-IR analysis of BSA fouled on ultrafiltration and microfiltration membranes. J Memb Sci 192: 201-207.
22. Tian J, Liu J, Hu Z, Chen X (2005) Interaction of wogonin with bovine serum albumin. Bioorg Med Chem 13: 4124-4129.
23. Kragh-Hansen U, Chuang VT, Otagiri M (2002) Practical aspects of the ligand-binding and enzymatic properties of human serum albumin. Biol Pharm Bull 25: 695-704.
24. Lakowicz JR (2007) Principles of fluorescence spectroscopy, Springer.
25. Maurya JK, Mir MUH, Singh UK, Maurya N, Dohare N, et al. (2015) Molecular investigation of the interaction between ionic liquid type gemini surfactant and lysozyme: A spectroscopic and computational approach. Biopolymer 103: 406-415.
26. Morris GM, Goodsell DS, Halliday RS, Huey R, Hart WE, et al. (1998) Automated docking using a Lamarckian genetic algorithm and an empirical binding free energy function. J Comput Chem 19: 1639-1662.
27. Ojha B, Das G (2010) The interaction of 5-(alkoxy)naphthalen-1-amine with bovine serum albumin and its effect on the conformation of protein. J Phys Chem B 114: 3979-3986.
28. Kandagal PB, Ashoka S, Seetharamappa J, Shaikh SM, Jadegoud Y, et al. (2006) Study of the interaction of an anticancer drug with human and bovine serum albumin: spectroscopic approach. J Pharm Biomed Anal 41: 393-399.
29. Ruiz CC, Hierrezuelo J, Peula-García J, Aguiar J (2008) Interaction between n-octyl-ß-D-thioglucopyranoside and bovine serum albumin. Open Macromolecules Journal 2: 6-18.
30. Airinei A, Tigoianu R, Rusu E, Dorohoi D (2011) Fluorescence quenching of anthracene by nitroaromatic compounds. Dig J Nanomater Biostruct 6: 1265-1272.
31. Shi X, Li X, Gui M, Zhou H, Yang R, Zhang H, Jin Y (2010) Studies on interaction between flavonoids and bovine serum albumin by spectral methods. Journal of Luminescence 130: 637-644.
32. Ross PD, Subramanian S (1981) Thermodynamics of protein association reactions: forces contributing to stability. Biochemistry 20: 3096-3102.
33. Das P, Mallick A, Chakrabarty A, Haldar B, Chattopadhyay N (2006) Effect of nanocavity confinement on the rotational relaxation dynamics: 3-acetyl-4-oxo-6,7-dihydro-12H indolo-[,3-a] quinolizine in micelles. J Chem Phys 125: 44516.
34. Mote US, Bhattar SL, Patil SR, Kolekar GB (2010) Interaction between felodipine and bovine serum albumin: fluorescence quenching study. Luminescence 25: 1-8.
35. Jash C, Payghan PV, Ghoshal N, Kumar GS (2014) Binding of the iminium and alkanolamine forms of sanguinarine to lysozyme: spectroscopic analysis, thermodynamics, and molecular modeling studies. Journal of Physical Chemistry B 118:13077-13091.
36. Bi S, Song D, Tian Y, Zhou X, Liu Z, et al. (2005) Molecular spectroscopic study on the interaction of tetracyclines with serum albumins. Spectrochim Acta A Mol Biomol Spectrosc 61: 629-636.
37. Fraiji LK, Hayes DM, Werner T (1992) Static and dynamic fluorescence quenching experiments for the physical chemistry laboratory. Journal of chemical education 69: 424.
38. Han XL, Mei P, Liu Y, Xiao Q, Jiang FL, et al. (2009) Binding interaction of quinclorac with bovine serum albumin: a biophysical study. Spectrochim Acta A Mol Biomol Spectrosc 74: 781-787.
39. Nahar S, Tajmir-Riahi H (1996) Complexation of heavy metal cations Hg, Cd, and Pb with proteins of PSII: evidence for metal–sulfur binding and protein conformational transition by FTIR spectroscopy. J Colloid Interface Sci 178: 648-656.
40. MacDonald GM, Barry BA (1992) Difference FT-IR study of a novel biochemical preparation of photosystem II. Biochemistry 31: 9848-9856.

41. Pavlidis IV, Gournis D, Papadopoulos GK, Stamatis H (2009) Lipases in water-in-ionic liquid microemulsions: Structural and activity studies. J Mol Catal B Enzym 60: 50-56.

42. Chen P, Tian H, Zhang L, Chang PR (2008) Structure and properties of soy protein plastics with e-caprolactone/glycerol as binary plasticizers. Industrial & Engineering Chemistry Research 47: 9389-9395.

43. Yang X, Wu D, Du Z, Li R, Chen X, et al. (2009) Spectroscopy study on the interaction of quercetin with collagen. J Agric Food Chem 57: 3431-3435.

44. Bouhekka A, Bürgi T (2012) In situ ATR-IR spectroscopy study of adsorbed protein: visible light denaturation of bovine serum albumin on TiO2. Appl Surf Sci 261: 369-374.

45. Shi X, Li D, Xie J, Wang S, Wu ZQ, et al. (2012) Spectroscopic investigation of the interactions between gold nanoparticles and bovine serum albumin. Chinese Science Bulletin 57: 1109-1115.

46. Ye F, An YG, Qin DZ, Yang L, She L, et al. (2007) Spectroscopic study on the effect of crystallization of the hydroxyapatite on the secondary structure of bovine serum albumin. Guang Pu Xue Yu Guang Pu Fen Xi 27: 321-324.

47. Bourassa P, Kanakis CD, Tarantilis P, Pollissiou MG, Tajmir-Riahi HA (2010) Resveratrol, genistein, and curcumin bind bovine serum albumin. J Phys Chem B 114: 3348-3354.

48. Bhattacharya B, Nakka S, Guruprasad L, Samanta A (2009) Interaction of bovine serum albumin with dipolar molecules: fluorescence and molecular docking studies. J Phys Chem B 113: 2143-2150.